

TREATED DIATOMITE FOR TOLUIDINE BLUE REMOVAL FROM WASTEWATER. IS IT WORTH IT?

ANDRADA S. MĂICĂNEANU^{a*}, RALUCA PLEȘA CHICINAȘ^b,
HOREA BEDELEAN^c

ABSTRACT: The adsorption of Toluidine Blue (TB) cationic dye was performed using raw and treated (thermal, chemical, thermo-chemical, ultrasonic) diatomite. Solid samples were characterized using X-ray diffraction (XRD), scanning electron microscopy (SEM), X-ray photoelectron spectroscopy (EDX), and Fourier Transformed Infrared Spectroscopy (FTIR). Adsorption experiments were performed in batch conditions ($20 \pm 2^\circ\text{C}$, 100 mg TB/L, 100 mL, 0.1 g adsorbent). The best sample proved to be the one thermally treated at 250°C for 2 h with an adsorption capacity of 7.97 mg/L and 77% removal efficiency. The regeneration process of the used diatomite was also performed (calcination, HCl, water), the most efficient was the one using water. Kinetic models (pseudo-first-, pseudo-second-order, liquid film, and intra-particle diffusion) were considered to describe the experimental data. The calculated data showed that liquid film diffusion might be rate-determining step in this case.

Keywords: diatomite, adsorption, toluidine blue, regeneration, kinetics

INTRODUCTION

Industrial activities such as textile, cosmetics, pulp and paper, plastic, paints, printing, leather, pharmaceuticals, food, and mineral processing are all discharging wastewaters with a high content of dyes [1,2]. Wastewater treatment, based on physical, chemical, or biological processes, such as coagulation, flotation, adsorption, chemical oxidation, filtration, ozonation, ion-exchange, and aerobic and anaerobic microbial degradation, were all

^a *Madia Department of Chemistry, Indiana University of Pennsylvania, Indiana, PA 15705, USA*

^b *Ana Aslan Technical College, 41 Decebal st., 400124, Cluj-Napoca, Romania*

^c *Department of Geology, Babes-Bolyai University, 1 M. Kogălniceanu st., 400048, Cluj-Napoca, Romania*

* *Corresponding author: sanda.maicaneanu@iup.edu*

considered for dye removal from wastewater. Between the available methods, adsorption has proven to be effective and convenient and activated carbon the adsorbent used with the best results. Due to the high costs involved in its regeneration, low-cost substitute materials were considered [1,3,4].

There are many studies which have shown that numerous natural and inexpensive materials were successfully applied in the removal of dyes from wastewaters, such as coal, wood powder, lignin, shale oil ash, zeolite, perlite, clay minerals, diatomite, activated slag, activated carbon, fly ash, and agricultural wastes [3-5].

The most important property of an adsorbent is the surface area and structure. Any solid material with a microporous structure and a large surface area can be used as adsorbent. Diatomite is one of the materials which fulfils these conditions [6,7].

Diatomite is a fine, siliceous natural rock, composed mainly by microscopic frustules (skeletal remains) of silica microfossils of dead diatoms, radiolaria, and sponges. Most diatoms are elongated (pennate diatoms), while others are round (centric diatoms). The main component of diatomite is amorphous silica ($\text{SiO}_2 \cdot n\text{H}_2\text{O}$). Sometimes the siliceous deposits may be pure, sometimes they are mixed with clay, carbonates, or organic matter. It's a pale-colored, soft, light-weight sedimentary rock, with 80-90% voids in its structure [6-8].

Diatomite has numerous physical and chemical properties that are important for the adsorption process, which include high porosity, high permeability, small particle size, high surface area, and low thermal conductivity. All these properties make diatomite a low-cost alternative to activated carbon, suitable for many industrial applications such as filtering and adsorption of organics and heavy metals from wastewater [6,9,10]. Diatomite surface is terminated by OH groups (will form hydrogen bonds with the adsorbate) and oxygen bridges, which act as adsorption sites [11].

Not many studies considered the influence of various treatments on adsorptive (organic compounds) properties of diatomite. Aivalioti et al. [12,13] studied BTEX, MTBE, and TAME adsorption on raw, thermally, chemically (acid), and both chemically and thermally treated diatomite, with the sample treated with HCl being the most effective [13]. Dye and printing wastewaters were used to test adsorptive properties of diatomite treated with HCl 5% followed by calcination at 500°C [14]. HF etching (various concentrations, time of reaction, temperatures) was proved to drastically change the porous structure of diatomite and therefore adsorptive properties towards methylene blue [15]. Thermo-chemical treated diatomite (H_2SO_4 5-6M, 900°C) was used

to remove methylene blue from aqueous solutions, two studies indicating that this type of treatment improves its performances as adsorbent [16,17]. Diatomite subjected to a NaOH treatment proved to improve its adsorptive properties towards methylene blue adsorption [18].

The aim of this study was to explore the use of Romanian pennate frustules diatomite as adsorbent for toluidine blue (TB) dye removal from aqueous solution and to decide if the treatments applied to the raw diatomite are justified. Reutilization of the spent diatomite after regeneration was also considered. As treatment applied to diatomite are likely to modify its porous structure, kinetic models (pseudo-first-, pseudo-second-order, liquid film, and intra-particle diffusion) were considered to describe the experimental data.

RESULTS AND DISCUSSION

Adsorbent characterization

The diatomitic ore from Minișu de Sus, the most important one in Romania, is located in the western part of the country, in Arad County. It is of Sarmatian age and it is positioned within the lower tuffaceous diatomitic complex. Diatomite layers are usually interbedded with clays, limestone as thin intercalations, as well as with silts, sands, and pyroclastic material. The diatomite from Minișu de Sus may be characterized as clayey diatomites as it contains some amounts of smectitic clays, whereas the presence of calcite or other carbonate mineral is negligible. The white-yellowish diatomite consists mainly of a mixture of small elongate frustules of pennate diatoms, clay minerals, and amorphous silica. The pennate type of diatoms gives the material superior technical properties, compared to those constituted from centric forms [8].

X-ray diffraction analyses performed on random powders indicate the presence of silica minerals as the main component (Figure 1). The highly crystalline peaks of cristobalite and quartz could be observed. The presence of biogenic opal A (amorphous silica) is indicated by a slightly broad reflexion centered at $2\theta=20-25^\circ$ [19] and well crystallized quartz. The quartz crystals are even allogenic, of a volcanogenic origin, or formed from the devitrified glass. Smectitic clay minerals (montmorillonite) and feldspars are also present but in small amounts.

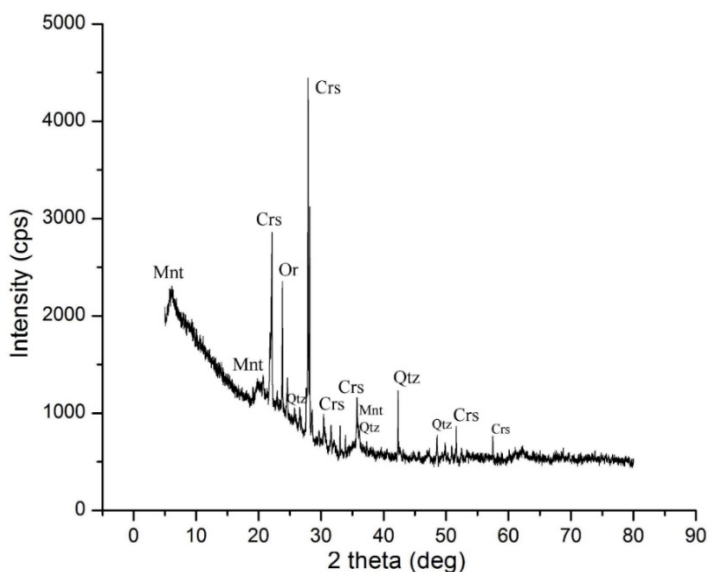


Figure 1. XRD pattern of raw diatomite (D) from Minișu de Sus (Arad County, Romania). Legend: Crs = cristobalite, Mnt = montmorillonite, Or = orthoclase, Qtz = quartz

SEM analysis provides data on the morphology of diatoms and on the porosity of the material. The images revealed the presence of the pennate frustules of diatoms with open-pores dispersed in clay matrix (Figure 2). The porous structure can be observed. Pores and open voids provide natural filtration and adsorption properties to the diatomaceous material.

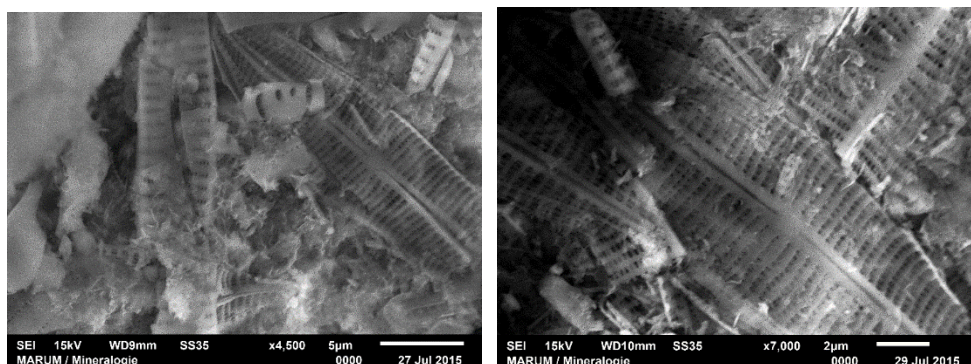


Figure 2. SEM images of raw diatomite (D) from Minișu de Sus (Arad County, Romania). Fragments of pennate diatoms frustules hosted in a clayey matrix.

The chemical composition of the diatomitic material varies, due to the lithological heterogeneity of the ore [8]. SiO_2 is the main oxide, between 65-76%, constituting the diatom frustules, opal-A is present in the cement, while detrital quartz and silicates (feldspar, clay minerals) are also present. Al_2O_3 has average values between 5-19 %, being found in feldspars and clay minerals. Fe_2O_3 is contained mainly by iron oxi-hydroxides and varies between 3-7%. CaO is in small amounts, between 2-6%. It is present in plagioclases, montmorillonite and probably in secondary carbonates. According to the $\text{SiO}_2:\text{Al}_2\text{O}_3$ ratio, the diatomites for Minișu de Sus belong to the clayey-type. From the EDX spectra of the considered diatomite sample (D) (Figure 3), the atomic elemental composition in wt. % was depicted as follows: 64.6 – O, 26.5 – Si, 5.69 – Al, 1.12 – Ca, 0.98 – Fe, 0.64 – Mg, 0.26 – Na and 0.15 – K (the difference up to 100% corresponds to gold used for sample preparation).

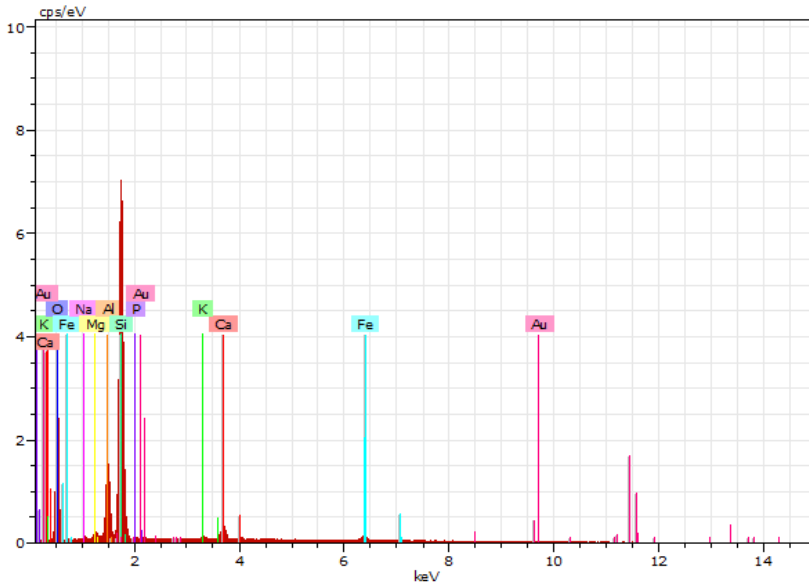


Figure 3. EDX spectra of raw diatomite (D) from Minișu de Sus (Arad County, Romania).

The FTIR spectra for raw diatomite and some of the treated samples (the ones which were giving the best results in terms of dye removal efficiencies) are presented in Figure 4. The main bands indicated the presence of diatomite specific peaks, Figure 4 and Table 1. All the samples present similar spectra with a slight increase in the intensity in case of thermal and thermo-chemical treated samples. The bands at $3625\text{-}3630\text{ cm}^{-1}$ are attributed

to Si-OH stretching. The bands in the 3440-3443 cm^{-1} range are characteristic to O-H stretching vibration, while the 1636 cm^{-1} band is characteristic to H-O-H bending of adsorbed water molecules. The 1093-1094, 795-797, and 467-468 cm^{-1} bands are characteristic to Si-O-Si asymmetric stretching, Si-O-Si symmetric stretching and Si-O-Si / Si-O-Al bending, respectively [20-23].

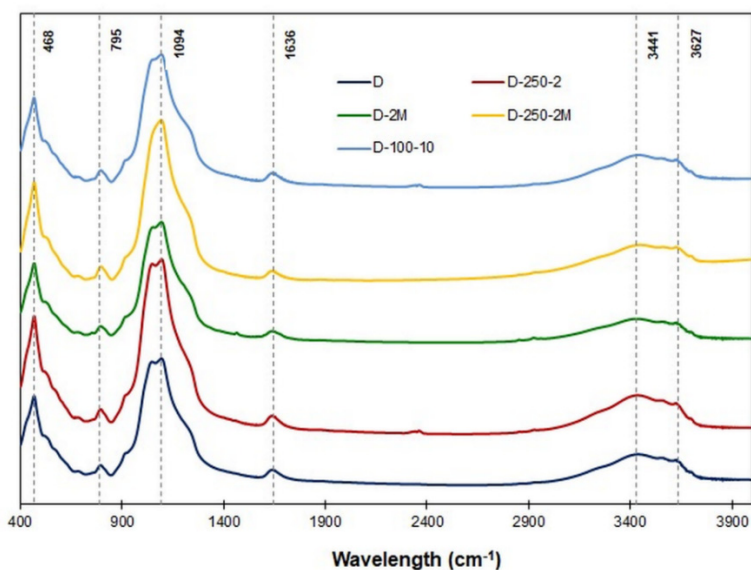


Figure 4. FTIR spectra of D, D-250-2, D-2M, D-250-2M, and D-100-10 diatomite samples.

Table 1. Most relevant infrared spectral bands of the D, D-250-2, D-2M, D-250-2M, and D-100-10 samples [20-23].

Sample	D	D-250-2	D-2M	D-250-2M	D-100-10	Assignment
Wavelength (cm^{-1})	468	467	468	467	467	Si-O-Si / Si-O-Al symmetric bending
	795	795	796	797	796	Si-O-Si symmetric stretching
	1094	1094	1094	1093	1094	Si-O-Si asymmetric stretching
	1636	1636	1636	1636	1636	H-O-H bending
	3441	3440	3440	3444	3443	O-H stretching
	3627	3626	3626	3625	3630	Si-OH stretching

Adsorption results

For each considered treatment applied to the raw diatomite sample, maximum removal efficiencies were considered and compared. In the case of thermally treated samples, Figure 5a, a small increase in removal efficiency, from 71 to 77%, was observed for D-250-2 sample. This fact might be attributed to the fact that as the temperature increases water is removed from the solid surface, making pores more accessible. Further increase of the temperature led to partial collapsing of the porous structure [24] and therefore to a decrease of the surface available for adsorption, hence a decrease of removal efficiency to 58% recorded for D-750-2 sample. When calcination time was increased from 1 to 4 hours at 500°C, the decrease in removal efficiency was constant irrespective to the calcination time (71 to 57%).

When chemical treatment was considered, Figure 5b, a slight increase in removal efficiency was observed for D-2M sample (from 71 to 76%), while with a further increase of the HCl concentration, D-4M sample, removal efficiency dropped to 67%. This decrease might be due to the reaction occurring between the acid and the metal oxides on the adsorbent surface, reaction products blocking the pores of the diatomite, thereby reducing adsorption efficiency [25].

Thermo-chemical treatment of the raw diatomite did not show a positive trend on improving its adsorption capacity, Figure 5c. The removal efficiency values decreased from 71 to 57% for D and D-750-2M, respectively.

In the case of ultrasonic treatment, increasing of power and treatment time led to the same trend in removal efficiency evolution, Figures 5d and 5e. The best results, with a removal efficiency of 76% were obtained in case of both D-100-10 and D-120-8 samples. Further increase of time (> 10 min) and power (> 120 W) could have as a result pores destruction and therefore a decrease in removal efficiency values. Between the best results obtained for various treatments, Figure 6, slight improvements in terms of removal efficiency by comparison with D sample were obtained just for D-250-2, D-2M, D-100-10, and D-120-8 samples.

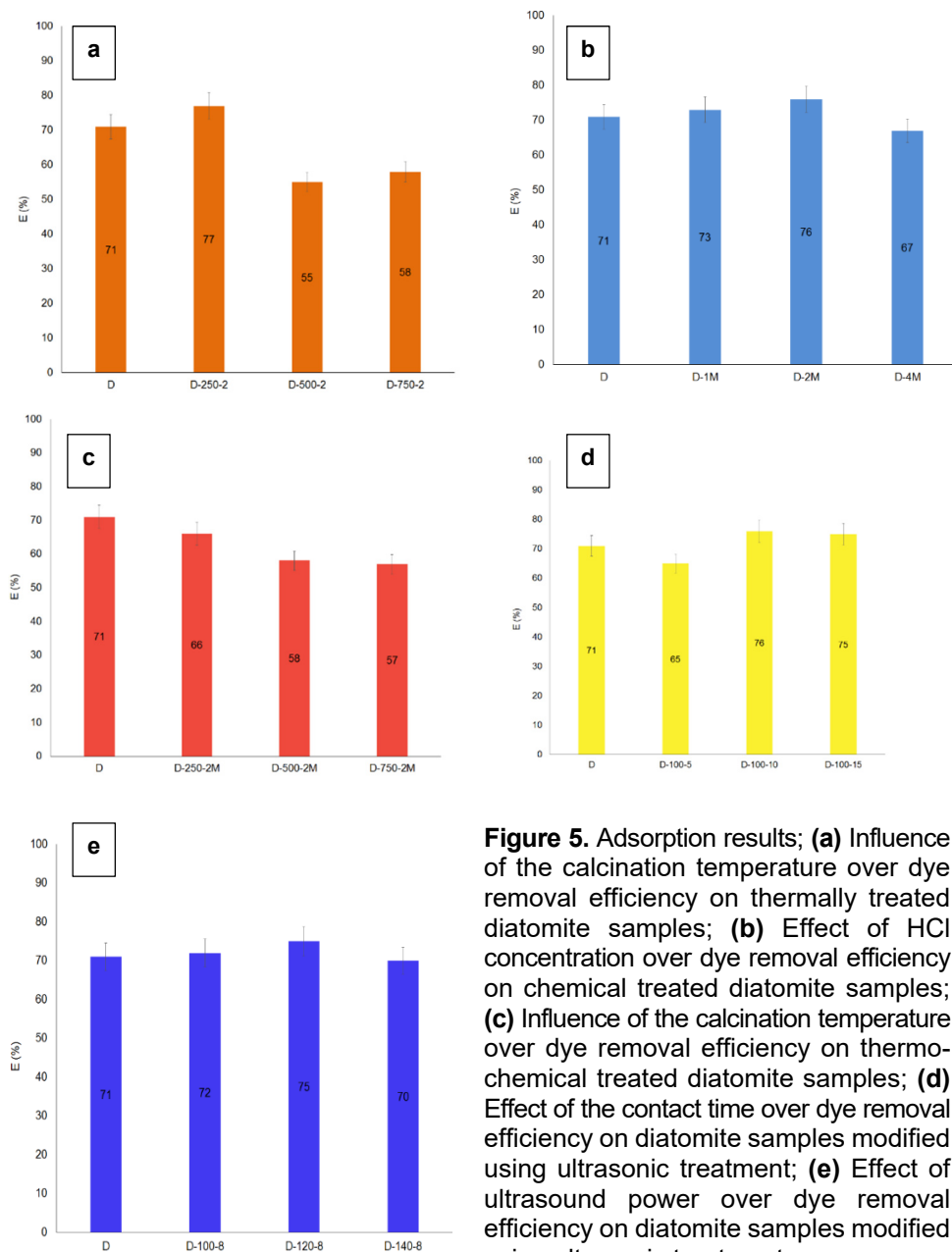


Figure 5. Adsorption results; **(a)** Influence of the calcination temperature over dye removal efficiency on thermally treated diatomite samples; **(b)** Effect of HCl concentration over dye removal efficiency on chemical treated diatomite samples; **(c)** Influence of the calcination temperature over dye removal efficiency on thermo-chemical treated diatomite samples; **(d)** Effect of the contact time over dye removal efficiency on diatomite samples modified using ultrasonic treatment; **(e)** Effect of ultrasound power over dye removal efficiency on diatomite samples modified using ultrasonic treatment.

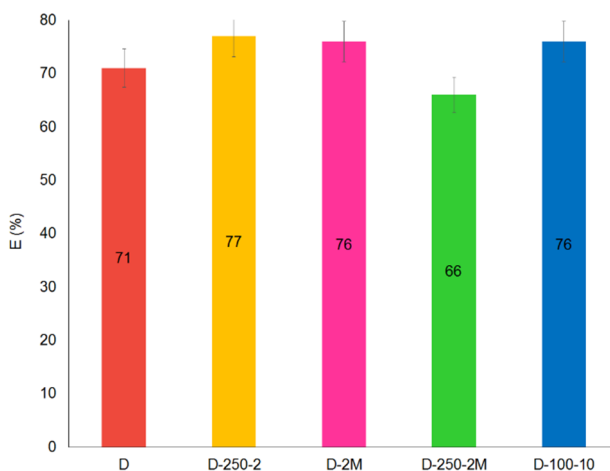


Figure 6. Comparison of the maximum removal efficiencies obtained for each considered treatment.

Adsorbent regeneration

The regeneration methods used on spent diatomite samples as described in the Experimental section, proved to have similar results when temperature and acid were used. Thermal treatment at 500°C and repeated contact with HCl led to a drastically decrease of removal efficiency (52%) after the third regeneration-adsorption cycle, Figure 7.

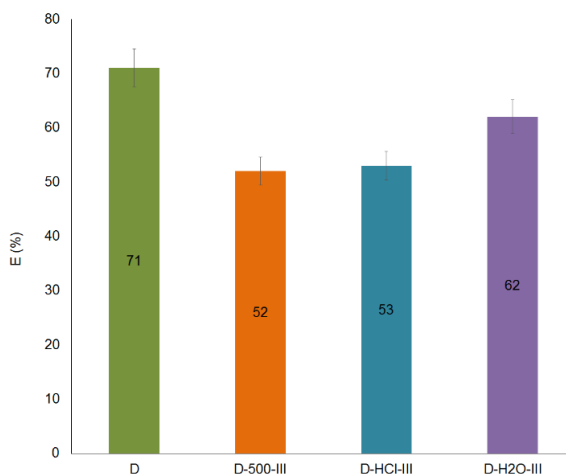


Figure 7. Effect of the regeneration method over dye removal efficiencies obtained after the third regeneration-adsorption cycle.

These two methods are quite expensive and have a high environmental impact. In the case of water, a slower decrease in removal efficiency was recorded, 69, 65, and 62% after the first, second, and third regeneration cycle, respectively. Depending on the dye concentration present in water and considering that diatomite is a low-cost material, usage up to 3-5 cycles with water as a regeneration agent could be a promising process for colored wastewater treatment. When studied only thermal regeneration (300-900°C), Auguedal et al. found that at 600°C, the adsorbed Red ETL dye was completely removed, and around 73% was restored after three regeneration cycles [26].

Adsorption kinetics

Several adsorption kinetic models, such as pseudo-first- (Lagergren), pseudo-second-order, liquid film, and intra-particle diffusion models, (equations are presented in Table 2), were used to test experimental data in order to investigate the adsorption mechanism and potential rate determining steps [27-30]. The pore diffusion coefficient, D (cm²/s) was also calculated (assuming a spherical geometry of the adsorbents – average size 0.1 cm) using the following equation [31,32]:

$$D = 0.003 \cdot \frac{r_0^2}{t_{0.5}} \quad (1)$$

Based on the pseudo-second-order model, $t_{0.5}$ was estimated using equation [32,33]:

$$t_{0.5} = \frac{1}{k_2 q_e} \quad (2)$$

Time evolution of TB concentration for D and D-250-2 samples, Figure 8, shows that the removal process takes place with a relatively small rate and the equilibrium was reached after about 300 min.

The results obtained for all considered models are presented in Table 2. The pore diffusion coefficients are 7.93×10^{-8} and 2.67×10^{-8} cm²/s for D and D-250-2, respectively, higher values than rate determining range ($10^{-11} - 10^{-13}$ cm²/s) [33]. Taking into consideration all the calculated values, regression coefficient (R^2) values, the fact that in the case of liquid film model the intercepts have values very close to 0 [34], Table 2, and also the shape of the time evolution curve (Figure 8), we have concluded that in this particular case, liquid film diffusion could be rate-determining step.

Table 2. Pseudo-first-, pseudo-second-order, intra-particle, and liquid film diffusion parameters for TB adsorption onto D and D-250-2 samples.

Diatomite sample	Pseudo-first-order				Pseudo-second-order		
	$\ln(q_e - q_t) = \ln q_e - k_2 \cdot t$ [27]				$\frac{t}{q_t} = \frac{1}{k_2 \cdot q_e^2} + \frac{t}{q_e}$ [28]		
	$q_{e,exp}$	k_1	$q_{e,cal}$	R^2	k_2	$q_{e,cal}$	R^2
D	7.39	0.0112	9.394	0.9525	3.0790	13.45	0.9816
D-250-2	7.97	0.0124	10.29	0.9335	5.0937	12.24	0.9945
	Intra-particle diffusion				Liquid film diffusion		
	$q_t = k_{ip} \cdot t^{0.5}$ [29]				$\ln(1 - F) = -k_{fd} \cdot t$ [30]		
D	0.5086	-1.1903	0.9966	0.0112	-0.2403	0.9525	
D-250-2	0.0119	1.6859	0.9518	0.0124	-0.2558	0.9335	

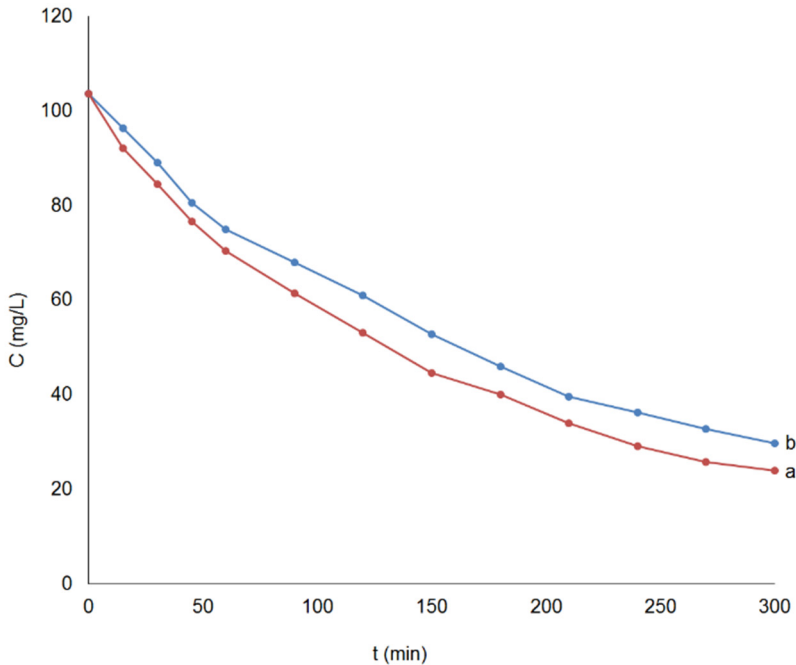


Figure 8. Time evolution of TB concentration for adsorption on (a) D and (b) D-250-2 diatomite samples.

CONCLUSIONS

A Romanian diatomite sample subjected to various treatments (thermal, chemical, thermo-chemical, and ultrasonic) was tested for the removal of toluidine blue cationic dye from aqueous solutions. XRD, FTIR, and SED-EDX analyses confirmed the siliceous nature of the diatomaceous material, presence of the pennate frustules of diatoms, and the small amount of impurities. Between the considered treatments applied to the raw diatomite, improvements in terms of adsorption capacity and removal efficiency were obtained in case of: D-250-s (7.97 mg/g and 77%), D-2M and D-120-8 (7.85 mg/g and 75%), and D-100-10 (7.93 mg/g and 76%) by comparison with D (7.39 mg/g and 71%). Regeneration of the diatomite samples was realized using thermal, acid, and water methods. The results showed that when the regeneration was realized with water, the smallest decrease in removal efficiency was obtained even after three regeneration-adsorption cycles (a drop of 13% by comparison with thermal regeneration where a 27% drop was recorded). The calculated data showed that liquid film diffusion might be rate-determining step in this case.

To answer the question from the title, besides the 2 h at 250°C treatment, the slight improvement in adsorption capacities and efficiency obtained for all the other treatments do not justify the costs of these treatments.

EXPERIMENTAL

Materials

Diatomite sample (raw diatomite) collected from Minișul de Sus deposit, Arad County, Romania was used as an adsorbent in this study. Characterization of diatomite was realized using X-ray diffraction (XRD), scanning electron microscopy (SEM), X-ray photoelectron spectroscopy (EDX), and Fourier Transformed Infrared Spectroscopy (FTIR).

Toluidine Blue, $C_{15}H_{16}ClN_3S \cdot 0.5 ZnCl_2$, 373.97 g/mol, TB (Sigma Aldrich) was used as model dye molecules for the adsorption processes. A stock solution of 1000 mg/L was used to prepare the desired concentration (100 mg/L) solution.

Adsorbent preparation

Thermal, chemical, thermo-chemical, and ultrasonic treatments were applied to the raw diatomite sample. A total of 17 samples have been prepared as described below.

Raw diatomite was first subjected to a grinding process, followed by size separation to obtain the 0.6-1.0 mm fraction, which was further used throughout the experiments. Raw diatomite was then washed a few times with distilled water in order to remove fine particles and dried at 105°C for 24h.

Thermal treatment was realized through calcination at different temperatures in 250-750°C interval for 1, 2, and 4 h, modified after Aivalioti et al. [12,13]. Five thermal modified samples were obtained, Table 3.

Chemical treatment was performed using HCl solution of different concentrations (1 M, 2 M, and 4 M), modified after Zhang et al. [25]. Raw diatomite and acid solution were contacted at room temperature under mechanical stirring (300 rpm) for 3 h at a solid:liquid ratio of 1:10. The obtained samples were separated from the acid solution, thoroughly washed with distilled water until no chlorine was detected (AgNO_3 0.01 N) and dried at 105°C for 24 h, Table 3.

Thermo-chemical treatment was achieved using a chemical treated sample (HCl 2M, as described above) subsequently calcined at 250, 500, and 750°C for 2 h, Table 3.

Ultrasonic treatment, modified after Zhang et al. [25], was realized using power settings in 100-180 W interval and contact time of 5 to 15 min as follows: 20 g of raw diatomite and 100 mL distilled water were added in a glass beaker, which was then placed in an ultrasonic bath at room temperature at an established power and time interval. The solid was recovered by settling, washed with distilled water and dried at 105°C for 24 h. Six samples were thus obtained, Table 3.

Adsorbent characterization

XRD analyses of diatomite samples were performed using a D8 ADVANCE Bruker diffractometer, $\text{CuK}\alpha$ anticathode. The diffractograms were recorded from 5° to 80°, 2 θ degree. The analytic conditions were 40 kV, 40 mA, and a step of 0.02 degrees/min.

SEM-EDX analyses were performed using a JEOL JSM-6510 and Bruker EDX equipment. Prior to scanning, the diatomite sample was mounted on a stainless-steel slab with double stick tape and coated with a thin layer of gold in high vacuum condition.

FTIR analyses were performed on dried samples prepared by encapsulating 1.2 mg of finely grounded particles in 300 mg of KBr. Infrared spectra were obtained using a JASCO 615 FTIR spectrometer 400-4000 cm^{-1} (resolution, 2 cm^{-1}).

Adsorption experiments

TB adsorption process was conducted in batch conditions, in a thermostated batch reactor placed on a shaker (50 rpm), using 1 g adsorbent (0.6-1.0 mm grain size), 100 mL dye solution (100 mg/L), at $20 \pm 2^\circ\text{C}$. Working conditions were selected based on preliminary experimental results. Dye concentration from solution was determined using a UV-Vis Jenway 6305 spectrophotometer (calibration curve 2-10 mg/L) at the maximum absorption wavelength of $\lambda_{\text{TB}} = 633 \text{ nm}$. Experiments were conducted in the same conditions for all diatomite samples considered. The evolution and effectiveness of the dye adsorption process were evaluated by means of the amount of dye adsorbed, q (mg/g) and removal efficiency, E (%) [35].

Adsorbent regeneration

Although diatomite is a low-cost material, there might be instances when regeneration and/or dye recovery will be required. Therefore, this study considered the potential reuse of the spent diatomite, proposing three regeneration methods for the raw diatomite, namely: thermal, acid, and water, Table 4. In case of acid (HCl) and water (distilled) regeneration, diatomite was contacted with the liquid using a solid:liquid ratio of 1:10, under continuous stirring (shaker) at 50 rpm for 5 h. Three regeneration-adsorption cycles were realized in each case.

Table 3. Diatomite treatments and samples labeling.

Treatment	Label	Parameter		
Raw	D	grinding / size separation / washing		
Thermal		Temperature ($^\circ\text{C}$)		Time (h)
	D-250-2	250		2
	D-500-1	500		1
	D-500-2	500		2
	D-500-4	500		4
Chemical		HCl concentration (M)		
	D-1M	1		
	D-2M	2		
	D-4M	4		
Thermo-chemical		Temperature ($^\circ\text{C}$)	Time (h)	HCl concentration (M)
	D-250-2M	250	2	2
	D-500-2M	500	2	2
	D-750-2M	750	2	2

Ultrasonic		Power (W)	Time (min)
	D-100-5	100	5
	D-100-10	100	10
	D-100-15	100	15
	D-100-8	100	8
	D-120-8	120	8
	D-140-8	140	8

Table 4. Spent diatomite regeneration; type, samples labeling, and removal efficiencies.

Regeneration	Label	Regeneration parameters	Regeneration-adsorption cycle	E (%)
Raw	D	-		71
Thermal	D-500-I	500°C, 2 h	I	58
	D-500-II		II	54
	D-500-III		III	52
Acid	D-HCl-I	HCl 2M, 5 h	I	65
	D-HCl-II		II	55
	D-HCl-III		III	53
Water	D-H ₂ O-I	H ₂ O, 50°C, 5 h	I	69
	D-H ₂ O-II		II	65
	D-H ₂ O-III		III	62

Abbreviations

C_e – concentration of dye at equilibrium (mg/L)

D – pore diffusion coefficient (cm^2/s)

E – removal efficiency (%)

F – fraction attainment at equilibrium ($=q_t/q_e$)

k_1 – pseudo-first-order rate constant (1/min)

k_2 – pseudo-second-order rate constant (g/mg·min)

k_{fd} – liquid film diffusion rate constant (1/min)

k_{ip} – intra-particle diffusion rate constant ($\text{mg/g}\cdot\text{min}^{0.5}$)

q – the amount of dye adsorbed (mg/g)

q_e – the amount of dye adsorbed at equilibrium – adsorption capacity (mg/g)

$q_{e,exp}$ – the experimental amount of dye adsorbed at equilibrium (mg/g)

$q_{e,cal}$ – the calculated amount of dye adsorbed at equilibrium (mg/g)

q_t – the amount of dye adsorbed at time t (mg/g)

r_0 – diatomite grain diameter (cm)

t – time (min)

$t_{0.5}$ – time for half adsorption (s)

REFERENCES

1. E. Erdem; G. Çölgeçen; R. Donat; *J. Colloid Interf. Sci.*, **2005**, 282, 314-319.
2. M. Toor; B. Jin; S. Dai; V. Vimonses; *J. Ind. Eng. Chem.*, **2015**, 21, 653-661.
3. J.X. Lin; S.L. Zhan; M.H. Fang; X.Q. Qian; *J. Porous Mat.* **2007**, 14, 449-455.
4. E. Bulut, M. Özacar; I. A. Şengil; *J. Hazard. Mater.*, **2008**, 154, 613-622.
5. L. Lian; L. Guo; C. Guo; *J. Hazard. Mater.*, **2009**, 161, 126-131.
6. P. Moslehi; P. Nahid; *Int. J. Eng., Transactions B: Applications*, **2007**, 20, 141-146.
7. M.A.M.M. Khraisheh; Y.S. Al-Degs; W.A.M. Mcminn; *Chem. Eng. J.*, **2004**, 99, 177-184.
8. V.C. Brana; C. Avramescu; I. Călugăru; *Substanțe minerale nemetalifere*, Editura Tehnică, București, **1986**, pp. 133-135.
9. A. Sari; D. Çitak; M. Tuzen; *Chem. Eng. J.*, **2010**, 162, 521-527.
10. M.A. Al-Ghouti; M.A.M. Khraisheh; S.J. Allen; M.N. Ahmad; *J. Environ. Manage.*, **2003**, 69, 229-238.
11. M.A.M.M. Khraisheh; M.A. Al-Ghouti; S.J. Allen; M.N. Ahmad; *Water Res.*, **2005**, 39, 922-932.
12. M. Aivalioti; I. Vamvasakis; E. Gidarako; *J. Hazard. Mater.*, **2010**, 178, 136-143.
13. M. Aivalioti; P. Papoulias; A. Kousaiti; E. Gidaracos; *J. Hazard. Mater.*, **2012** 207-208, 117-127.
14. W. Zhaolun; Y. Yuxiang; Q. Xuping; Z. Jianbo; C. Yaru; N. Linxi; *Environ. Chem. Lett.*, **2005**, 3, 33-37.
15. W.-T. Tsai; C.-W. Lai; K.-J. Hsien; *J. Colloid Interf. Sci.*, **2006**, 297, 749-754.
16. Z. Al-Qodah; W.K. Lafi; Z. Al-Anber; M. Al-Shannag; A. Harahsheh; *Desalination*, **2007**, 217, 212-224.
17. E.A. Mohamed; A.Q. Selim; A.M. Zayed; S. Komarneni; M. Mobarak; M.K. Seliem; *J. Colloid Interf. Sci.*, **2019**, 534, 408-419.
18. J. Zhang Jian; Q. Ping; M. Niu; H. Shi; N. Li; *Appl. Clay Sci*, **2013**, 83-84, 12-16.
19. S.D.J. Inglethorpe; *Industrial minerals, Laboratory manual: Diatomite*, BGS Technical Report WG/92/39, **1993**.
20. N. Inchaurredo; J. Font; C.P. Ramos; P. Haure; *Appl. Catal. B*, **2016**, 181, 481-494.
21. H. Liang; S. Zhou; Y. Chen; F. Zhou; C. Yan; *J. Taiwan Inst. Chem. Eng.*, **2015**, 49, 105-112.
22. W. Tang; K. Qiu; P. Zhang; X. Yuan; *Appl. Surf. Sci.*, **2016**, 362, 545-550.
23. T. Qian; J. Li; X. Min; Y. Deng; W. Guan; L. Ning; *Energ. Convers. Manage.*, **2015**, 98, 34-45.
24. S.S. Ibrahim; A.Q. Selim; *Physicochem. Probl. Mi.*, **2012**, 48(2), 413-424.
25. G.Zhang; D. Cai; M. Wang; C. Zhang; J. Zhang; Z. Wu; *Micropor. Mesopor. Mat.*, **2013**, 165, 106-112.
26. H. Aguedal; A. Iddou; A. Aziz; A. Shishkin; J. Ločs; T. Juhna; *Int. J. Environ. Sci. Technol.*, **2019**, 16, 113-124.
27. S. Lagergren; *Kungl. Svenska Vetenskapskad. Handl.*, **1898**, 24, 1-39.

28. Y.S. Ho; G. McKay; *Process Saf. Environ.*, **1998**, *76*, 332-340.
29. W.J. Weber; J.C. Morris; *J. Sanit. Eng. Div. ASCE*, **1963**, *89*, 31-60.
30. G.E. Boyd; A.W. Adamson; L.S. Myers Jr.; *J. Am. Chem. Soc.*, **1947**, *69*, 2836-2848.
31. V. Srihari; A. Das; *Desalination*, **2008**, *225*, 220-234.
32. X.-Y. Pang; F. Gong; *E-J. Chem.*, **2008**, *5*, 802-809.
33. L.C. Cotet; A. Măicăneanu; C.I. Fort; V. Danciu; *Sep. Sci. Technol.*, **2013**, *48*, 2649-2658.
34. N. Caliskan; A.R. Kul; S. Alkan; E.G. Sogut; I. Alacabey, *J. Hazard. Mater.*, **2011**, *193*, 27-.
35. D.M. Gligor; A. Măicăneanu, Applications of Clay Minerals in Electrochemistry and Wastewater Treatment, in *Clay: Types, Properties and Uses*, J. P. Humphrey, D.E. Boyd) Eds.; Nova Science Publishers Inc., New York, **2011**, Chapter 1, pp. 1-62.

